Journal of Chromatography A, 1217 (2010) 7265–7274

Contents lists available at ScienceDirect

Journal of Chromatography A

journal homepage: www.elsevier.com/locate/chroma

Ion-exchange chromatographic protein refolding

Esteban J. Freydell[a], Luuk van der Wielen[a], Michel Eppink[b,1], Marcel Ottens[a,*]

[a] Department of Biotechnology, Delft University of Technology, Delft, The Netherlands
[b] Biotechnology Operations, N.V. Organon, Schering-Plough, Oss, The Netherlands

ARTICLE INFO

Article history:
Received 18 June 2010
Received in revised form 3 September 2010
Accepted 14 September 2010
Available online 19 September 2010

Keywords:
Ion-exchange chromatography
Protein refolding
Fractional surface coverage
Matrix assisted refolding

ABSTRACT

The application of ion-exchange (IEX) chromatography to protein refolding (IExR) has been successfully proven, as supported by various studies using different model proteins, ion-exchange media and flow configurations. Ion-exchange refolding offers a relatively high degree of process intensification, represented by the possibility of performing protein refolding, product purification and product concentration, in one unit operation. Besides its high degree of process intensification, IExR offers an additional set of key advantages including: spatial isolation of the bound protein molecules and the controllable change in chemical composition using gradients. Despite of the acknowledgement of the former advantages, the lack of mechanistic understanding on how they influence the process performance of the ion-exchange refolding reactor, limits the ability to exploit them in order to optimize the performance of the unit. This paper presents a quantitative analysis that assesses the effect that the spatial isolation and the urea gradient, have on the IExR performance, judged on the basis of the refolding yield (Y_N) and the fractional mass recovery ($f_{Prot,Rec}$). Additionally, this work discusses the effect of the protein load, the protein loading state (i.e., native, denatured, denatured and reduced (D&R)) and the adsorbent type on $f_{Prot,Rec}$. The presented work shows: (1) that the protein load has a direct effect on $f_{Prot,Rec}$, and the magnitude of this effect depends on the loading state of the protein solution and the adsorbent type; (2) that irrespectively of the type of adsorbent used, the saturation capacity of a denatured protein is less than the native protein and that this difference can be linked to differences in accessible binding surface area; (3) that there is a clear correlation between fractional surface coverage (θ) and $f_{Prot,Rec}$, indicating that the former could serve as a good descriptor to assess spatial isolation, and (4) that the urea gradient has a direct link with the variations on the refolding yield, and this link can be quantitatively estimated using as descriptor the urea gradient slope (ξ). Overall, the information provided in this paper aims at the eventual development of rational design or selection strategies of ion-exchange media for the satisfactory and successful refolding of a target protein.

1. Introduction

Developments attained in recombinant DNA technology have significantly changed the way valuable proteins are produced today. Proteins that used to be purified from human fluids, animal or plant tissue can now be produced in large quantities using for example *Escherichia coli* (*E. coli*). As an expression system *E. coli* offers several advantages including (1) its molecular genetics are well understood, meaning that its genome can be modified with ease; (2) relatively inexpensive culturing procedures and (3) high fermentation yields [1–3]. One important limitation of this expression system though, is that the over expression of certain gene sequences leads to the accumulation of the product in an inactive, insoluble aggregate known as inclusion body (IB). To obtain the soluble and bio-active (native) product, two process steps are required and these are (1) inclusion bodies (IBs) solubilization and (2) protein refolding. IBs solubilization is usually done using a solution containing chaotropes (e.g., urea, guanidine hydrochloride), reducing agents (e.g., dithiothreitol, β-mercaptoethanol, etc.) and alkaline pH. This cocktail disrupts the intermolecular interactions holding the aggregated protein, releasing the product in a denatured and reduced (D&R) soluble form. Optimal solubilization conditions should provide maximum protein solubility, minimizing the fraction of soluble aggregates formed and maximizing the fraction of soluble denatured and reduced monomer product [4–7]. Protein refolding is achieved by decreasing the concentration of chaotropes and reducing agents in the concentrated protein solution, allowing the soluble protein to refold and to form its disulphide bonds. This change in chemical composition is basically a buffer exchange step that can either be attained by direct dilution or using liquid chromatography (chromatographic refolding).

* Corresponding author. Tel.: +31 15 2782151; fax: +31 15 2782355.
E-mail address: m.ottens@tudelft.nl (M. Ottens).
[1] Current address: Synthon N.V., Nijmegen, The Netherlands.

0021-9673/$ – see front matter © 2010 Elsevier B.V. All rights reserved.
doi:10.1016/j.chroma.2010.09.044

Chromatographic protein refolding offers a relatively high degree of process intensification, represented by the possibilities of performing: (a) protein refolding, (b) a controllable change in chemical composition, attained using gradients, (c) product purification and (d) product concentration, in one single unit operation. Chromatographic refolding has been successfully conducted using hydrophobic interaction chromatography (HIC) [8–10], size-exclusion chromatography (SEC) [11,12], immobilized metal affinity chromatography (IMAC) [13,14], and ion-exchange chromatography (IEX) [15–17].

Ion-exchange refolding (IExR) was probably first reported by Creighton [17], who showed that (1) a urea denatured protein could be reversibly bound to an ion-exchange resin, (2) the denaturant (i.e. urea) could be removed using a gradient, while keeping the protein bound inducing refolding and disulfide bond formation and (3) using a salt gradient, the refolded bound protein could be eluted, obtaining it in a relatively pure denaturant free fraction. Ever since, IExR has gained interest in the scientific community most likely due to reasons such as: (1) ion-exchange chromatography is widely used as a purification unit in the biopharmaceutical industry, thus IExR could be easily implemented into current processes; (2) compared to SEC, IEX chromatography offers high loading capacities and the possibility to concentrate the product during elution, using a salt gradient; (3) compared to HIC, the urea denatured protein can be easily bound to the IEX resin at relatively low salt concentrations, which is certainly not the case for HIC refolding and (4) protein–protein interactions are presumably mitigated as a result of the spatial isolation obtained upon the binding of the protein to the IEX resin, decreasing protein aggregation, positively affecting the refolding yield. The approach presented by Creighton has been, through the years, modified to include for example a concomitant pH, urea and salt gradient that has successfully been applied to refold lysozyme on a cation-exchanger [18,19] and iron superoxide dismutase (Fe-SOD) on an anion-exchanger [20]. More recently, using a no-flow incubation period IExR has successfully been applied to refold bovine serum albumin (BSA) [15] and α-fetoprotein (AFP) [21], demonstrating that IExR is well suitable to refold relatively complex proteins, as the latter two examples have 16 and 17 disulfide bonds, respectively. Despite the proven versatility of IExR, represented by its successful application to the refolding of a range of proteins (e.g., lysozyme, BSA, Fe-SOD) using different flow configurations (e.g., single gradient, dual gradient, no-flow incubation), the contributions of its key advantages (the spatial isolation of the bound protein molecules and the controlled change in chemical composition) to the unit's performance have not yet been quantitatively assessed.

This paper presents a quantitative analysis that assesses the effect of the fractional surface coverage (θ), the slope of the urea gradient (ξ) and the load of denatured and reduced protein on the performance of IExR, judged on the basis of refolding yield (Y_N) and fractional mass recovery ($f_{Prot,Rec}$). Additionally, this study also discusses the effect of the resin backbone and the influence of the spacer length. Fractional surface coverage and the slope of the urea gradient quantitatively describe the degree of spatial isolation and urea gradient, respectively. Accordingly, these variables provide the possibility to assess the contribution of these key advantages to the unit's performance and to determine whether their contribution is positive or adverse. As distinct from the approach presented by Li et al. [18–20] the flow configuration used in this study, decouples the salt and the denaturant gradient, allowing the independent study of the effect of the chaotrope gradient. Our results show: (1) the strong correlation between $f_{Prot,Rec}$ and fractional surface coverage and how this correlation is influenced by the loading state of the protein (e.g., native, denatured, denatured and reduced) and the backbone of the adsorbent; (2) the effect that the mass loaded of denatured and reduced (D&R) protein has on Y_N and $f_{Prot,Rec}$, and how the loading state of the protein affects the magnitude of this effect; and (3) the effect of slope of the urea gradient (ξ) on Y_N and $f_{Prot,Rec}$.

2. Materials and methods

2.1. Materials

Two model proteins were used in this study. The first was a fusion protein (FP) that has 117 amino acids, a molecular weight of 12,710 g mol^{-1}, three disulfide bonds, no free cysteines and a theoretical isoelectric point (p*I*) of 7.64 (based on its primary sequence). The protein was obtained in the form of inclusion bodies and was provided by Shering-Plough (Oss, the Netherlands). Based on its isoelectric point this model protein was used for the anion-exchange refolding experiments. The second model protein was lysozyme, purchased as L6876 from Sigma–Aldrich (Zwijndrecht, The Netherlands). Lysozyme has 129 amino acids, a molecular weight of 14,307 g mol^{-1} [22], four disulfide bonds [23], no free cysteines and a theoretical isoelectric point of 11.35 [24]. Based on its p*I* this model protein was used for the cation-exchange refolding experiments.

All the columns used for the ion-exchange refolding experiments were pre-packed columns, with a packed bed volume (V_C) of 1 ml and were purchased from GE-Healthcare (Uppsala, Sweden), these columns were: RESOURCE Q (V_C = 1 ml), RESOURCE 15S (V_C = 1 ml), Hi-Trap SPFF and Hi-Trap SPXL. The SOURCE ion-exchange media is based on porous particles made from polystyrene-divinyl benzene (PS-DVB) and substituted with quaternary ammonium (Q) or methyl sulfonate (S) groups, attached to the matrix via hydrophilic spacer arms following the hydrophilization of the polymeric base matrix. Hydrophilization of PS/DVB and acrylic polymers, may be obtained by grafting a hydrophilic oligomer of polymer to pendant vinyl groups located on the particle surface [25]. The Hi-Trap columns are packed with Sepharose Fast Flow (FF) media and Sepharose XL media. The Sepharose FF media is made of particles with a macroporous gel structure, with a neutral hydrophilicity, based on chains of agarose that are arranged in bundles [26]. The matrix is made of 6% agarose, highly cross-linked. Sepharose XL media is based on the same structure as the Sepharose FF media, however for this media the ionic ligands are bound to a long, approximately 40 kDa in molecular size [27], dextran chain grafted onto the agarose matrix prior to its functionalization, resulting in the functionalization of both the agarose matrix and the dextran chain [27].

Analytical size-exclusion of the fractions collected during the IExR experiments, was done using a Superdex 75 10/300 pre-packed gel filtration column, purchased from GE-Healthcare (Uppsala, Sweden). All chromatographic separations were performed on an ÄKTA explorer 10 equipped with the UNICORN software version 5.01 from GE Healthcare (Uppsala, Sweden).

All chemicals used were at least reagent grade purity or higher. Urea, DL-Dithiothreitol (DTT) and Guanidine-HCL (GuHCL) were purchased from Sigma–Aldrich (Zwijndrecht, The Netherlands). Sodium hydrogen carbonate, sodium hydroxide, sodium chloride and tris-(hydroxymethyl)-aminomethane (Tris) were purchased from JT.Baker (Deventer, The Netherlands). Acetone, ethylenediamine tetra acetic acid (EDTA), and hydrochloric acid were purchased from Merck (Schiphol-Rijk, The Netherlands). All solutions were prepared using water purified by Milli-Q Ultrapure Water Purification System from Millipore (Amsterdam, The Netherlands) and were vacuum filtered through a 0.22 μm pore size membrane filter from Pall (Portsmouth, Hampshire, United Kingdom).

Table 1
Solutions used for the anion-exchange refolding (AExR) experiments.

Buffer	Urea (M)	NaCl (mM)	Tris (mM)	$NaHCO_3$ (mM)	EDTA (mM)	pH
A11	0.5	–	50	20	0.2	10.5
B1	4	–	50	20	0.2	10.5
B2	0.5	1000	50	20	0.2	10.5

2.2. Protein quantification

The concentration of soluble protein was estimated using a BCA protein assay purchased from Fisher Scientific (Landsmeer, The Netherlands). Bovine serum albumin (BSA) was employed as a standard to estimate the total protein concentration of the fractions from the anion-exchange refolding experiments. Lysozyme was used as the standard to the estimate the total protein concentration in the fractions collected from the cation-exchange experiments.

2.3. Quantification of the native fusion protein

The refolded fusion protein was digested using trypsin in order to obtain the mature monomer. The digestion was done using an enzyme to substrate ratio, of 1:300 (mg:mg) [28,29]. The samples were incubated for 30 min and 25 °C using a thermomixer comfort from Eppendorf (Amsterdam, The Netherlands). The reaction was quenched by diluting the samples with a 100 mM HCL solution. The concentration of active protein was determined using reversed phase HPLC and a calibration line constructed using human insulin as standard [30].

2.4. Inclusion bodies solubilization

The inclusion bodies were solubilized in solubilization buffer (4 M urea/25 mM DTT/10 mM $NaHCO_3$/0.1 mM EDTA; pH 10.5) [4]. Solutions of various concentrations were prepared diluting the concentrated denatured and reduced protein solution with solubilization buffer.

2.5. Preparation of lysozyme solutions

Lysozyme in a native form was prepared in a solution of 50 mM Tris-HCL, pH 8.7. Denatured not reduced (DNR) lysozyme was prepared in a solution of 8 M urea/50 mM Tris, pH 8.7. Denatured and reduced (D&R) lysozyme was prepared in a solution of 8 M urea/100 mM DTT/50 mM Tris/pH 8.7 [18].

2.6. Analytical size-exclusion chromatography

Analytical SEC was used to estimate the amount of monomers and high-molecular weight aggregates present in the fractions collected from the IExR experiments. The analysis was conducted using a Superdex 75 10/300, at a flow rate of 0.5 ml min^{-1} and an injection volume of 0.2 ml. Prior to the analysis the column was calibrated using aprotinin (6500 Da), ribonuclease A (13,700 Da), carbonic anhydrase (29,000 Da) and conalbumin (75,000 Da). The columns void volumes, inter-particle volume and total volume, were determined with pulses on blue-dextran and acetone, respectively.

2.7. Isotherm measurements

Adsorption isotherms were determined for lysozyme under native and denaturing conditions (i.e., lysozyme in 8 M urea), for the Hi-Trap SP and the RESOURCE 15S columns. The isotherms were measured by frontal analysis (FA) [31] and the breakthrough curves (BTCs) were analyzed according to the approach presented by Gritti et al. [32]. The adsorbed protein concentration (q^*) in equilibrium with the feed concentration (C) was determined with Eq. (1).

$$q* = \frac{C(V_{eq} - V_0)}{V_C} \quad (1)$$

where V_{eq} represent the volume of the equivalent area [32], V_0 is the inter-particle void volume, V_C represent the packed bed volume, and C is the concentration of the feeding solution.

2.8. Anion-exchange refolding

Anion-exchange refolding (AExR) experiments were done using the Resource-Q anion-exchanger and the fusion protein. These experiments evaluated the effect of the slope of the denaturant gradient and the load of denatured and reduced protein on the refolding yield and the fractional mass recovery. Table 1 presents the list of buffers used and Fig. 1 presents the schematic representation of the flow scheme, indicating the different stages (e.g., equilibration, loading, etc.). The AExR experiments were performed as follows. The column was first equilibrated for 10 column volumes (CVs) with buffer B1 (Table 1), at 2 ml min^{-1}. Subsequently, a feed pulse of 1 ml, containing the denatured and reduced protein, at a concentration of 1 mg ml^{-1} was injected. The column was thereafter washed for 5 CVs with buffer B1. Next, the urea concentration was decreased using a linear gradient, exchanging buffer B1 for buffer A11 in 20 CVs. This gradient was operated at a flow rate selected to achieve the desired gradient slope (ξ). The slopes used were 0.35, 0.10 and 0.03 mol l^{-1} min^{-1}, obtained using the flow rates (ϕ_V) 2, 0.57 and 0.17 ml min^{-1}, and Eq. (2).

$$\xi = \frac{(C_{Urea,Init} - C_{Urea,End})}{\Delta CV} \cdot \frac{\phi_V}{V_C} \quad (2)$$

where ξ represents the gradient slope, $C_{Urea,Init}$ represents the urea concentration at the beginning of the gradient, $C_{Urea,End}$ represents the urea concentration at the end of the gradient, ΔCV represent the gradient's length, ϕ_V represents the flow rate and V_C represents the packed bed volume.

Following the urea gradient, the column was washed for another 5 CVs with buffer A11. Then, the bound protein was eluted using a sodium chloride (NaCl) gradient. This gradient was done at 2 ml min^{-1}, in 10 CVs, exchanging buffer A11 for buffer B2 (Table 1).

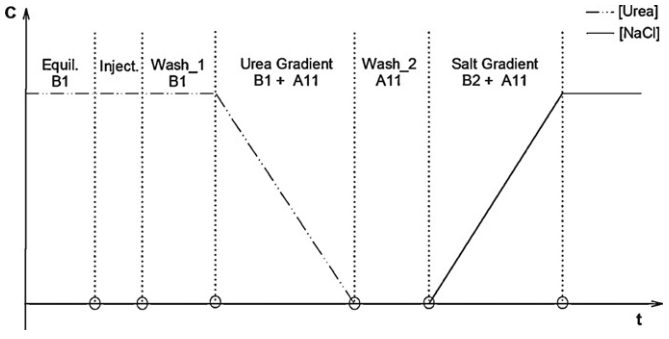

Fig. 1. Schematic representation of the flow scheme used for the anion-exchange refolding (AExR) experiments. Dash–dot line: urea concentration. Solid thick line: sodium chloride concentration. Equil: equilibration block; Inject: injection block; B1: buffer B1 (Table 1); A11: buffer A11 (Table 1); B2: buffer B2 (Table 1).

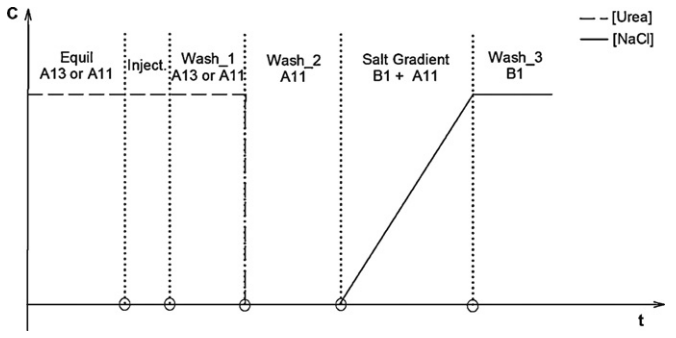

Fig. 2. Schematic representation of the flow scheme used for the cation-exchange refolding (CExR) experiments. Dash-line: urea concentration. Solid-thick line: sodium chloride concentration. Equil: equilibration block; Inject: injection block. A13, A11, B1 are the buffers used (see Table 2).

The column was then washed for another 5 CVs with buffer B2. Finally, the column was rinsed with milli-Q water for 5 CVs, regenerated using a 3 M guanidine hydrochloride (GnHCL) solution for 5 CVs and finally rinsed for 5 CVs with milli-Q water; all these steps were done at 2 ml min^{-1}.

During the AExR experiments the effect of the gradient slope (ξ), on the refolding yield (Y_N) and the fractional mass recovery, was studied at a fixed denatured and reduced protein load of 1 mg. The effect of the denatured and reduced protein load was studied at a fixed gradient slope of 0.10 mol l^{-1} min^{-1}, and for a D&R protein load ranging from 1 to 4 mg of protein.

2.9. Cation-exchange refolding

Cation-exchange experiments were done to study the effect of the denatured and reduced protein load, the backbone of the adsorbent and the spacer length on the fractional mass recovery. These experiments were done using the following strong cation-exchangers: RESOURCE 15S, Hi-trap SPFF and Hi-trap SPXL. The effect of the backbone was assessed by comparing the data obtained using the relatively hydrophilic backbone of the SOURCE adsorbent, based on hydrophilized PS/DVB, against the data obtained using the Sepharose adsorbents (SPFF, SPXL), whose backbone is based on cross-linked agarose. The effect of the spacer or the lack-thereof was studied by comparing the data obtained from the experiments with the SPFF and SPXL adsorbents, as both adsorbents have the same backbone and the same functional group. All these experiments were done using lysozyme as the model protein. Additionally, these experiments also evaluated the effect of the loading state of the protein. By loading state it is meant: native lysozyme, denatured lysozyme or denatured and reduced lysozyme. These loading states were generated dissolving lysozyme on buffers with or without urea and with urea and DTT (Section 2.5). All these experiments were done using a lysozyme feed concentration raging from 0.5 to 4.0 mg ml^{-1} and a fixed loading volume of 1 ml.

Fig. 2 presents the schematic representation of the flow scheme used for the CExR experiments, indicating the various blocks (e.g., equilibration, injection, etc.) and Table 2 presents the list of buffers used. The CExR experiments were done as follows. The column was first equilibrated for 12 CVs with buffer A13 (Table 2), for the experiments with either denatured or D&R lysozyme, or with buffer A11 (Table 1) for the experiments with native lysozyme. Subsequently, a feed pulse of 0.5 ml, containing either native, denatured or D&R lysozyme, was injected. Next, the column was washed with the equilibration buffer for 5 CVs. Thereafter, the mobile phase composition was changed on a step fashion (Wash_2, Fig. 2), going from buffer A13 to A11 in the experiments done with denatured or D&R lysozyme. For those experiments with native lysozyme no such mobile phase change took place, as for these experiments buffer A11 was used in the blocks equilibration, injection, Wash_1 and Wash_2 (Fig. 2). Right after block Wash_2 (Fig. 2), the bound protein was eluted with a linear sodium chloride gradient, changing the mobile phase composition from A13 or A11 to buffer B1 in 10 CVs. Then the column was washed with buffer B1 for 5 CVs. Finally, the column was rinsed with milli-Q water for 5 CVs, regenerated using a 3 M GnHCL solution for 5 CVs and finally rinsed for 5 CVs with milli-Q water. All the blocks on the flow scheme were executed at 1 ml min^{-1}.

Table 2
Solutions used for the cation-exchange refolding (CExR) experiments.

Buffer	Urea (M)	NaCl (M)	Tris (mM)	pH
A13	8	–	50	8.7
[a]A11	0	–	50	8.7
B1	0	1	50	8.7

[a] Buffer A11 was used, in place of buffer A13, for the experiments using native lysozyme .

2.10. Isotherm modeling

The isotherm data determined for lysozyme, under native and denaturing conditions, was analyzed using two mechanistic models, namely the Langmuir model and the Fowler model. The Langmuir model is commonly used to analyze adsorption data obtained on homogeneous surfaces and preferably under conditions where the fractional surface coverage (θ) is less than 0.10 [31]. The model assumptions include: the solute gives monolayer coverage and the bound solutes do not interact with each other in the monolayer. The Langmuir model is presented in Eq. (3).

$$q^* = \frac{bq_S C}{1 + bC} \tag{3}$$

where C represents the liquid concentration in equilibrium with the adsorbed concentration q^*, q_S is the saturation capacity of the stationary phase and b is a numerical coefficient related to the affinity of the solute for the binding surface.

The Fowler model was conceived as a model to correct for the first-order deviations of the Langmuir model, assuming that the bound solutes may interact while bound to the homogeneous surface [31]. Eqs. (4a) and (4b) describe the Fowler model.

$$bCe^{-\chi\theta} = \frac{\theta}{1-\theta} \tag{4a}$$

$$\theta = \frac{q^*}{q_S} \tag{4b}$$

where χ represents the interaction energy and θ represents the fractional surface coverage. The interaction parameter (χ) describes weak interactions between bound and incoming solute molecules.

2.11. Parameter estimation

The parameters of the isotherm models, i.e., Langmuir and Fowler, were estimated using a non-linear least squares algorithm programmed and solved in MATLAB R2007b. The objective function, minimized by the algorithm, was based on the method of Marquardt, as presented in Guiochon et al. [31]. The objective function is presented in Eq. (5). To solve Fowler's model, the optimization routine was constraint for $1 < \chi < 4$, because in this range the model has physical meaning.

$$f(x) = \sqrt{\frac{1}{N_D - P}\sum_{i-1}^{n}\left(\frac{q^*_{exp,i} - q^*_{mod,i}(x)}{q^*_{exp,i}}\right)^2} \tag{5}$$

where N_D represents the number of data points, P represents the number of parameters of the model, $q^*_{exp,i}$ represent the experimental adsorbed concentration, $q^*_{mod,i}$ represent the modeled adsorbed concentration, n is the number of elements of the concentration vectors, and x represent the vector of the model parameters.

2.12. Performance indicators

2.12.1. Fractional mass recovery

The fractional mass recovery ($f_{Prot,Rec}$) is defined as the total mass of protein recovered in the elution, divided by the total mass of protein injected to the ion-exchanger and it was calculated using:

$$f_{Prot,Rec} = \frac{V_{EPool} C_{Prot,E}}{V_{inj} C_{Prot,feed}} \quad (6)$$

where $f_{Prot,Rec}$ represent the fractional mass recovery, V_{EPool} represent the volume of the elution pool, V_{inj} represent the injection volume, $C_{Prot,E}$ is the total protein concentration in the elution pool and $C_{Prot,feed}$ is the total protein concentration fed to the column. For those experiments, were denatured and reduced (D&R) protein was used $C_{prot,feed} = C_{f,D\&R}$. Where $C_{f,D\&R}$ represent the feed concentration of denatured and reduced protein.

2.12.2. Refolding yield

The refolding yield (Y_N) is defined as the amount of active product formed per amount of denatured and reduced protein loaded to the column and it was calculated as follows:

$$Y_{N,IExR} = \frac{V_{MPool} C_{NPool}}{V_{inj} C_{f,D\&R}} \quad (7)$$

where V_{MPool} represent the volume of the pool carrying the native product, C_{NPool} is the concentration of native protein in the pool.

2.12.3. Volumetric productivity

The volumetric productivity of a chromatographic refolding reactor is defined as the amount of product (i.e., native protein) produced per unit time per volume of chromatographic medium

$$Pr_{IExR} = \frac{C_{f,D\&R} V_{inj}}{t_{cycle} V_C} Y_{N,IExR} \quad (8)$$

where $C_{f,D\&R}$ is the feed concentration of denatured and reduced protein, V_{inj} is the injection volume, t_{cycle} is the cycle time, V_C is the packed bed volume and $Y_{N,IExR}$ is the ion-exchange refolding yield.

3. Results and discussion

3.1. Adsorption behavior under denaturing and native conditions

Changes in the protein structure, such as the disruption of the tertiary and/or secondary structures, have been shown to have a strong influence in the adsorption behavior of proteins onto surfaces [33], and thus these changes will have a direct influence in the saturation capacity of the ion-exchanger and the affinity of a given protein for the surface of the adsorbent. Changes in protein structure may occur as a result of, for example, the disruption of hydrogen bonding occurring due to the action of a chaotropic agent (e.g., urea, GuHCL). To assess the effect of such structural changes on the adsorption behavior, adsorption experiments using native lysozyme, denatured lysozyme and the ion-exchangers Source 15S and Sepharose SPFF were done. The results of these experiments are presented in Fig. 3. Fig. 3A and B presents the adsorption isotherm of lysozyme under denaturing and non-denaturing (native) conditions, respectively. The isotherms were measured by frontal analysis (FA). From the data in Fig. 3A and B the following observations are evident: (1) the Sepharose SPFF has a higher capacity for

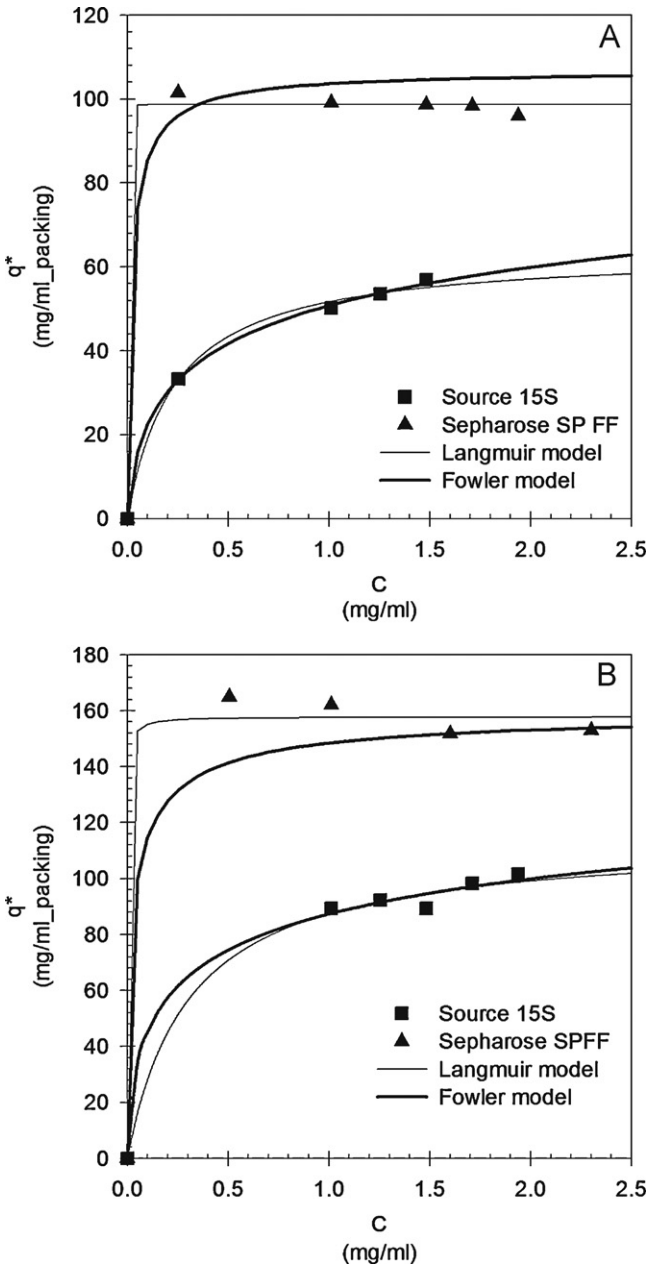

Fig. 3. Adsorption isotherms of lysozyme loaded in a denatured (A) and native (B) state, to the adsorbents Source 15S (■) and Sepharose SPFF (▲). Solid thin line: Langmuir model (Eq. (3)); solid thick line: Fowler model (Eqs. (4a) and (4b)). The parameters of the models, estimated with the aid of Eq. (5), are presented in Table 3.

lysozyme than the Source 15S media, for both native and denaturing conditions and (2) the saturation capacity under native conditions is higher than under denaturing conditions, regardless of the type of adsorbent use. The latter behavior seems to be protein independent, as similar observations using native and denatured and reduced α-lactalbumin, adsorbed onto a Source Q IEX adsorbent, have been reported [16]. The relatively low saturation capacity, exhibited by the denatured lysozyme compared to the native lysozyme, might be reasonably explained by a change in the accessible binding surface area, as this has been shown to be directly related to the molecule's dimensions [34,35]. In essence, molecules of different sizes have access to different fractions of the pore volume of a given adsorbent, affecting their accessibility to the binding surface. Basically, a large molecule will have access to less biding surface area than a small molecule. Denatured lysozyme

Table 3
Isotherm parameters determined for lysozyme adsorbed, under native and denaturing conditions, to the adsorbents Source 15S and Sepharose SPFF.

Adsorbent	Feeding condition	Fowler model				Langmuir model		
		q_S (mg/ml packing)	b (ml/mg)	x	[a]Obj.fun	q_S (mg/ml packing)	b (ml/mg)	[a]Obj.fun
Source 15S	Native	149.77	14.43	4	0.047	114.40	3.25	0.040
	Denatured	105.47	6.38	4	0.023	63.80	4.26	0.032
Sepharose SPFF	Native	159.03	200.21	2.84	0.165	157.80	600	0.052
	Denatured	106.82	100	1.15	0.105	98.67	64832	0.022

[a] Obj.fun: Objective function given by Eq. (5).

is a larger molecule than native lysozyme [36], hence it has less access to the binding surface, explaining its relatively low saturation capacity. The saturation capacities of denatured and reduced lysozyme, for both the Source 15S and the Sepharose SPFF, are presented in Table 3. The data in Table 3 was derived from the analysis of the adsorption data with the Fowler model (Eqs. (4a) and (4b)) and the Langmuir model (Eq. (3)). It is interesting to point out from the data in Table 3, that both models predict practically a change in saturation capacity (denatured vs. native) of equal magnitude. This finding supports the hypothesis that the change in saturation capacity (q_S) is caused by the differences in accessibility of denatured and native lysozyme to the binding surface, as both ion-exchange materials have been shown to have very close mean pore radius and phase ratio functions [35].

Lastly, although both models are in principle suitable for the analysis of the adsorption data, as shown by their ability to represent the experimental trend (Fig. 3A and B), the Langmuir model is not adequate for the presented case, as the fractional surface coverage (θ) in these experiments goes beyond 0.10 [31]. Therefore, the Fowler model will be used in follow up discussions.

3.2. Effect of the protein load and the loading state on the fractional mass recovery ($f_{Prot,Rec}$) and the refolding yield (Y_N)

Protein load is an important operational variable in ion-exchange refolding (IExR) because it directly affects the volumetric productivity of the reactor (Eq. (8)), which is an important performance indicator. And thus, its effect on the fractional mass recovery (Eq. (6)) and the refolding yield (Eq. (7)) of the IExR unit was studied using both the cation-exchange (CExR) and the anion-exchange (AExR) model systems. Additionally, the effect of the loading state (i.e., denatured, D&R) was also investigated, since during ion-exchange refolding the protein might be fed either as denatured protein or as denatured and reduced protein, depending on whether a reducing agent (e.g., DTT, β-mercaptoethanol) was used or not during the solubilization of the inclusion bodies.

Fig. 4 presents the results from the CExR experiments. These series of experiments were done using native lysozyme (▲), denatured lysozyme (●), D&R lysozyme (■) and the cation exchangers Source 15S (Fig. 4A), Sepharose SPFF (Fig. 4B) and Sepharose SPXL (Fig. 4C). The first question addressed, using the data from the CExR experiments, was whether the protein load had an effect on the fractional mass recovery ($f_{Prot,Rec}$). The data in Fig. 4 show that the protein load does affect the $f_{Prot,Rec}$ and this effect seems to be adverse. Furthermore, these data show that this effect depends on the type of cation exchanger and on the loading state of the protein (i.e., native, denatured, D&R). The effect of the type of cation exchanger seems to be linked to the adsorbent's backbone; this claim is supported by the comparison of Fig. 4A and B. This comparison shows that the effect of the protein load on the $f_{Prot,Rec}$ is more pronounced on the hydrophilic backbone of the Source 15S media (Fig. 4A) than on the neutrally hydrophilic backbone of the Sepharose media (Fig. 4B and C). It is important to point out from the data in Fig. 4A, that the effect of the protein load is relatively more pronounced for the native lysozyme, than for the denatured lysozyme. This behavior may be reasonably explained by the hydrophilic nature of the Source's backbone, since the native protein binds more tightly than the denatured protein, as the latter should have a higher hydrophobic surface area than the former as a result of the denaturation process.

The effect of the loading state is evident from the comparison of the experimental data corresponding to the D&R lysozyme (■) and the data from the native (▲) and denatured (●) lysozyme (Fig. 4A–C). From this comparison, it can be concluded that loading under D&R conditions results in the minimum fractional mass recovery, irrespectively of the amount loaded or the type of adsorbent use. To explain this finding, the following hypothesis is formulated, loading under D&R conditions results in the formation of a tightly bound layer of protein, insensible to the action of sodium chloride. Loading under D&R conditions means that the protein being fed comes with a high concentration of free thiolate anions (–S–), which are reactive species in nature. Since these species have a negative charge, their interaction with the negatively charged surface of the cation exchanger, is improbable. As a result, interactions between bound protein molecules and bound protein molecules with incoming protein molecules are likely to occur via the thiolate anion, forming inter-chain disulfide bonds. Additionally, hydrophobic interactions between protein molecules may also occur, as under D&R conditions the core of the protein molecules is fully exposed. As a result, a multilayer of protein forms on top of the adsorbent's surface, blocking the accessibility of the Na^+ (counter-ion) to the first layer of protein allegedly bound solely via ionic interactions with the adsorbent's ligands. This hypothesis is supported by the data presented in Fig. 4D. Fig. 4D presents a typical elution chromatogram obtained using the Hitrap SPFF column and a protein load of 0.5 mg. The data show that when lysozyme is loaded under native (Fig. 4D, dash–dot line) or denatured (Fig. 4D, solid thin line) conditions, elution with sodium chloride (NaCl) is feasible. However, elution with NaCl is inefficient when lysozyme is injected in a denatured and reduced form (Fig. 4D solid thick line), resulting in the elution of the protein during the regeneration with the 3 M guanidine hydrochloride solution.

Lastly, a comparison between the data in Fig. 4B and C, indicated that having a long spacer does not seem to bring an advantage, as the behavior of the data obtained with both the Sepharose SPFF and the Sepharose SPXL follows practically equal trends.

Up to this point the data have made clear the effect of the protein load on the fractional mass recovery, but what is its effect on the refolding yield? To address this question the AExR model system was used. Fig. 5 presents the results of the anion-exchange refolding experiments, obtained using the Source Q anion-exchange media, a fixed urea gradient slope (ξ) of 0.10 mol l^{-1} min^{-1} and the fusion protein. The fusion protein was fed to the column in a denatured and reduced state, as both urea and DTT were used for the efficient solubilization of the inclusion bodies [4]. Fig. 5A presents the AExR chromatograms, showing the three fractions collected (i.e., F1, F2, F3). The data show that the increase in loading resulted mostly in an increase of the peak area corresponding to fraction F3. Analysis

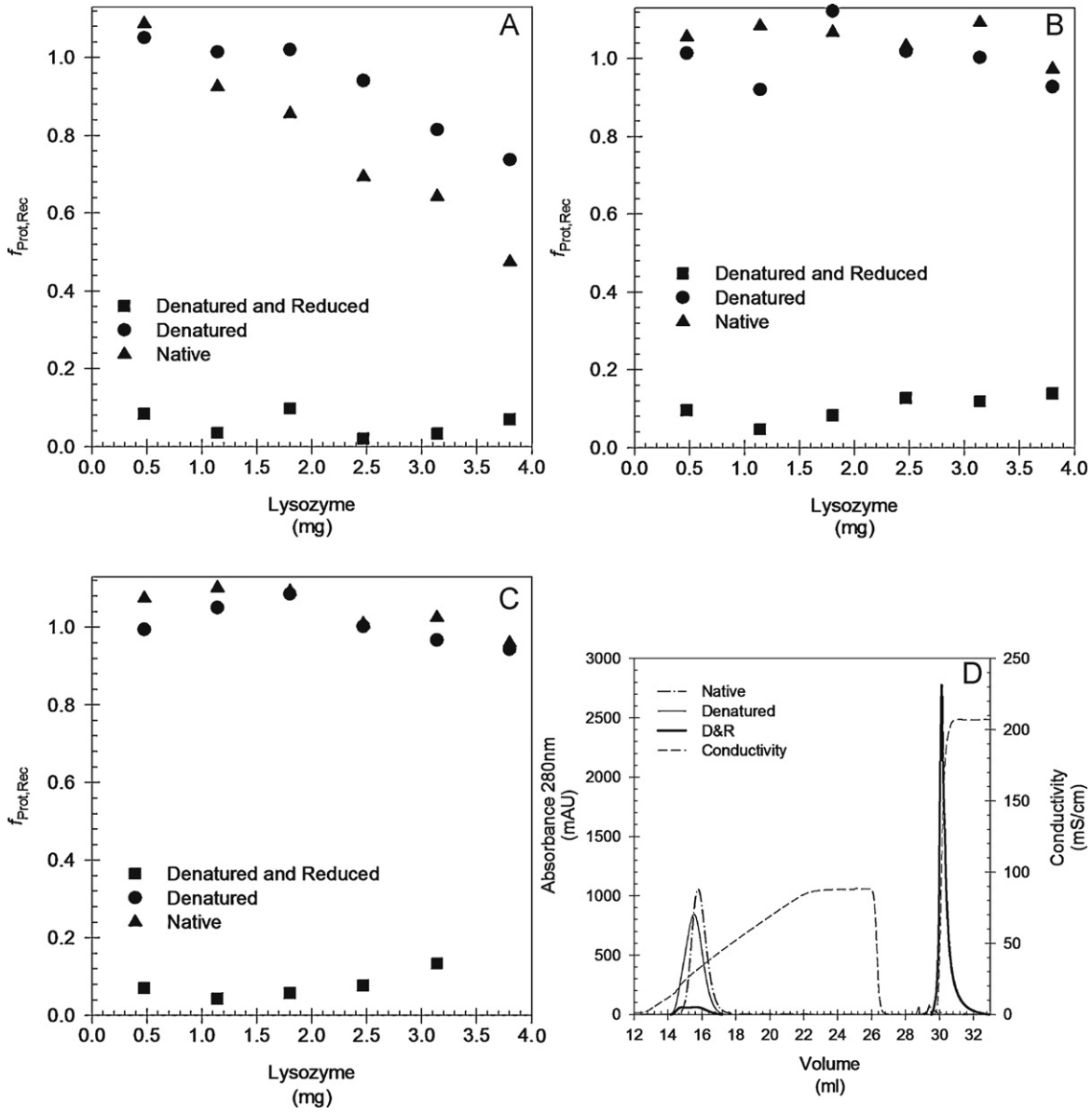

Fig. 4. Effect of the protein load and the protein feeding state (i.e., native, denatured, D&R) on the fractional mass recovery ($f_{Prot,Rec}$). The experiments were done using the cation-exchangers Source 15S (A), Sepharose SPFF (B), Sepharose SPXL (C) and lysozyme on a native (▲), denatured (●) and denatured and reduced (D&R) (■) state. (D) Typical elution chromatogram obtained during the CExR experiments; Column: HiTrap SPFF, load = 0.5 mg. Dash–dot–dash line: native lysozyme; solid thin line: denatured lysozyme; solid thick line: D&R lysozyme; dashed line: conductivity signal.

of the AExR fractions using analytical SEC (Fig. 5B), indicated that fraction F3 is predominantly composed of aggregated protein. The SEC analysis also revealed that the percentage of aggregated protein in fraction F3 correlates well with the protein load used during the AExR experiments (inset Fig. 5B), increasing as the protein load increases. This finding explains the adverse effect that the protein load had on the refolding yield of the AExR system, which is evident from the data in Table 4. Table 4 summarizes the results from the AExR experiments, indicating the effect of the protein load on the refolding yield and the fractional mass recovery of the AExR system. It is important to point out from the data in Table 4, that the effect of the protein load on the $f_{Prot,Rec}$ of the AExR system, is very similar to the effect measured during the CExR experiments, as in both systems increasing the protein load decreases the $f_{Prot,Rec}$. Thus, it is safe to say that protein load adversely affects the fractional mass recovery of ion-exchange refolding (IExR) systems. This claim is further supported by similar trends reported for a different model protein and using a different flow scheme configuration [15].

Finally, a comparison between the findings obtained from the AExR and CExR data and the reported data of the concomitant salt, pH, urea system [18,19], strongly suggested that endowing the elution buffer with a relatively high urea concentration will likely increase the $f_{Prot,Rec}$ of the IExR system, loaded with D&R protein. This hypothesis was confirmed using the AExR model system by adding 4 M urea to the elution buffer, leading to a $f_{Prot,Rec} \geq 0.80$

Table 4
Effect of the protein load on the refolding yield and the fractional mass recovery of the anion-exchange model system.

[a]Load (mg protein/ml bed)	[b]Y_N	$f_{Prot,Rec}$
1	0.18	0.57
2	0.08	0.41
4	0.06	0.35

[a] The protein was loaded as denatured and reduced protein.
[b] Urea slope (ξ) fixed at 0.1 mol l^{-1} min^{-1}.

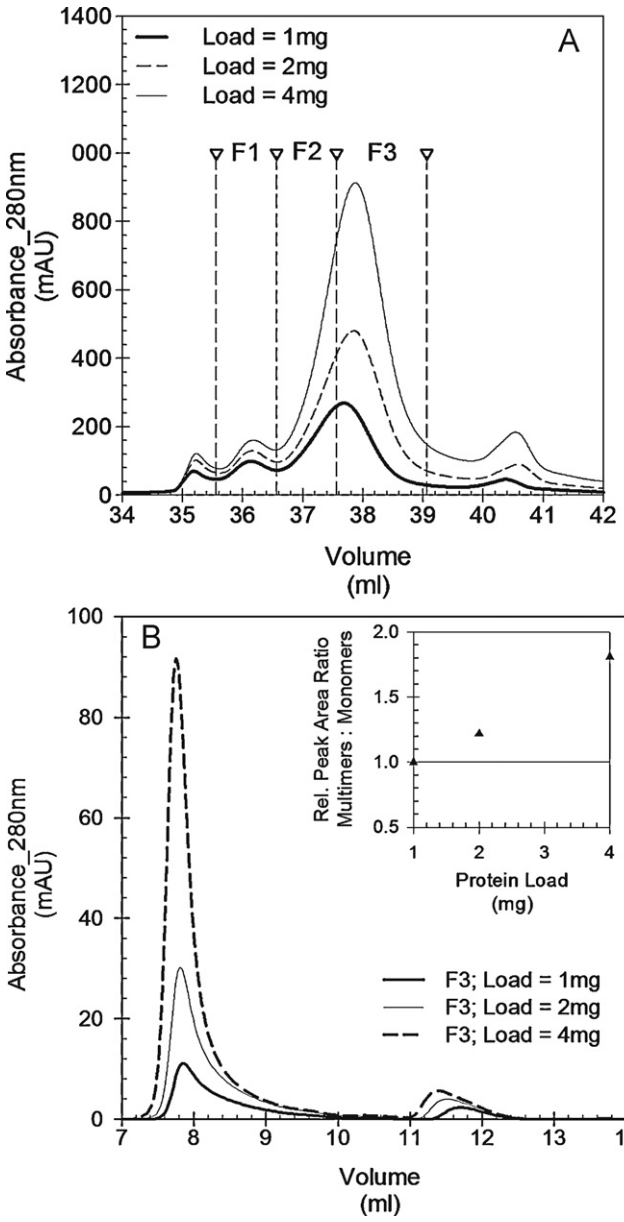

Fig. 5. Effect of the denatured and reduced (D&R) protein load on the elution chromatogram of the AExR model system. (A) Elution chromatogram of the AExR experiments. Solid thick line: load = 1 mg; short-dashed line: load = 2 mg; solid thin line: Load = 4 mg. All AExR experiments were done with a urea gradient slope (ξ) = 0.10 mol l^{-1} min^{-1}. (B) SEC analysis of the AExR fractions. Short-dash line: fraction F3 from the AExR experiment done at a load of 4 mg; solid thin line: fraction F3 from the AExR experiment done at a load of 2 mg; solid thick line: fraction F3 from the AExR experiment done at a load of 1 mg. The inset presents the correlation between relative peak area ratio, determined as the peak area of the monomer divided as the peak area of the aggregates, and the AExR protein load.

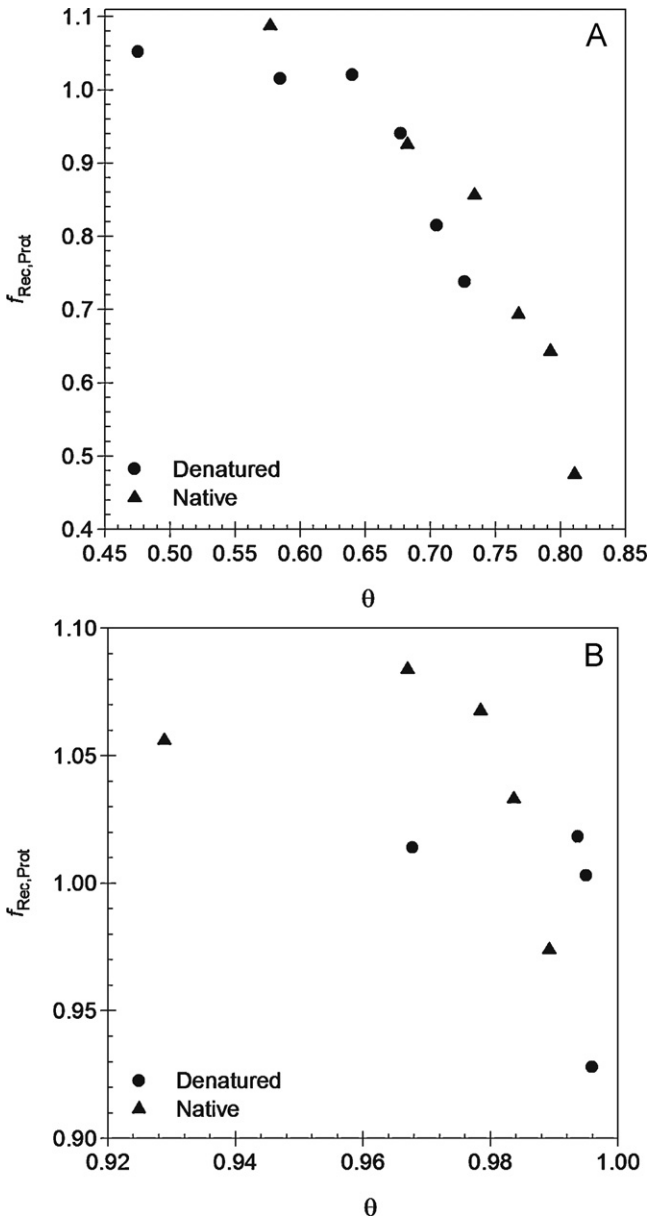

Fig. 6. Correlation between fractional surface coverage (θ) and fractional mass recovery ($f_{Rec,Prot}$), for native (▲) and denatured (●) lysozyme loaded to the adsorbents Source 15S (A) and Sepharose SPFF (B).

(data not shown). This hypothesis was also confirmed by Langenhof et al. [15], who reported a $f_{Prot,Rec} \approx 0.90$ when the elution buffer of his AExR model system was endowed with a 8 M urea concentration. Thus, it can be concluded that adding urea to the elution buffer will likely increase the $f_{Prot,Rec}$, however the concentration of urea to be used should be determined for each system, as this value should minimally comply with the following requirements: (1) the concentration of urea in the protein fractions should be less than the critical urea concentration, as being close or above this value will likely result in a decrease in protein activity; and (2) the concentration of urea leaving the IExR unit should be compatible with the subsequent processing steps.

3.3. Fractional surface coverage (θ) and its relation to the fractional mass recovery ($f_{Prot,Rec}$)

Spatial isolation, resulting from the binding of the protein molecules to the adsorbent's surface, has been suggested to be one of the key advantages of IExR systems [37]. In principle, a high spatial isolation should prevent protein-protein interactions, hence decreasing the chance of protein aggregation. Although theoretically accepted, attempts to quantitatively assess spatial isolation, in the context of ion-exchange protein refolding, have not been reported yet. Here, the fractional surface coverage (θ) (Eq. (4b)) has been chosen as the variable to quantify the degree of spatial isolation. Fig. 6 presents the correlation between fractional surface coverage (θ) and fractional mass recovery ($f_{Prot,Rec}$), for native lysozyme (▲) and denatured lysozyme (●), estimated for the Source 15S (Fig. 6A) and the Sepharose SPFF (Fig. 6B) ion-exchange media. Overall, the data indicates a clear correlation between the two variables, showing how as the fractional surface coverage increases,

beyond a certain threshold, the fractional mass recovery will commence to descend. A reasonable interpretation of this behavior is that as θ increases, the spatial isolation of the bound molecules decreases, increasing the chance of the bound molecules to interact with each-other and with incoming molecules. These interactions may lead then to the formation of a tightly bound protein layer, of variable thickness, that blocks the access of Na^+ (counter-ion) to the first layer of protein, allegedly bound to the surface of the adsorbent solely via ionic interactions with the ligands; resulting in a decrease of the $f_{Prot,Rec}$ owing to an inefficient protein elution during the salt gradient. Lastly, from the data in Fig. 6A and B is evident that the correlation between θ and $f_{Prot,Rec}$ is more pronounced for the adsorbent Source 15S than for the adsorbent Sepharose SPFF. The reason for this difference is at this point unknown, however it does suggest that the physicochemical properties of the adsorbent may have a contribution to the behavior of the data, and raises the following questions (1) what are the properties of the adsorbent involved? And (2) what is their contribution to the behavior of the data? These questions, fall out of the scope of the presented work and are material for follow up research.

3.4. Effect of the urea gradient on the refolding yield (Y_N) and the fractional mass recovery ($f_{Rec,Prot}$)

In addition to the spatial isolation of the bound molecules, the ability to change the urea concentration around the protein, in a controllable manner using a gradient, is also a key advantage of ion-exchange refolding (IExR). It has been suggested that the ion-exchange refolding yield is positively influenced by a gradual change in the urea concentration [17], because such gradual change allegedly prevents the rapid collapse of the protein, favoring the formation of the native product [18,19]. Despite the different suggestions and hypotheses, a quantitative analysis indicating if there is a direct link between the urea gradient and the performance the of ion-exchange refolding unit, has not been reported yet. So far, the effect of the urea gradient has been reported using a concomitant urea, pH and salt gradient [18,19]. The data on these studies however, cannot be used to tease out the contribution of the urea gradient to the change in refolding yield, since the concentration of urea changes simultaneously with the salt concentration and the pH. In this study, the urea and the salt gradient were decoupled and the pH of the mobile phase was fixed, to investigate the effect of the urea gradient alone. As descriptor of the urea gradient, the urea gradient slope (ξ) was used and its definition is presented in Eq. (2). The experiments were done using the AExR model system and the conditions for these experiments are presented in Section 2.8. It is important to point out that these experiments were done at a fixed D&R protein load of 1 mg; this relatively low load was chosen as such because a low load decreases the fractional surface coverage, increases the fractional mass recovery and the refolding yield, as has been shown in previous sections of this paper.

Fig. 7A presents the elution chromatograms of the AExR experiments as a function of the urea gradient slope (ξ), showing the three distinct fractions that were collected. These fractions were analyzed by BCA to determine the total protein concentration, by RPHPLC to determine the amount of native protein, and by SEC to estimate the fraction of monomers and aggregates. Fig. 7B presents a typical SEC chromatogram resulting from the analysis of the AExR fractions, showing their composition in terms of monomers ($10.50 < V_e < 13.50$) and aggregates ($V_e < 10.50$). Table 5 presents the summary of the results, and from these data the following conclusions could be made: (1) the AEx refolding yield (Y_N) of the model protein is inversely proportional to the urea gradient slope (ξ), meaning that as ξ increases the Y_N decreases and vice versa; and (2) the contribution of the urea gradient slope to the fractional mass recovery ($f_{Rec,Prot}$) is negligible. The fact that

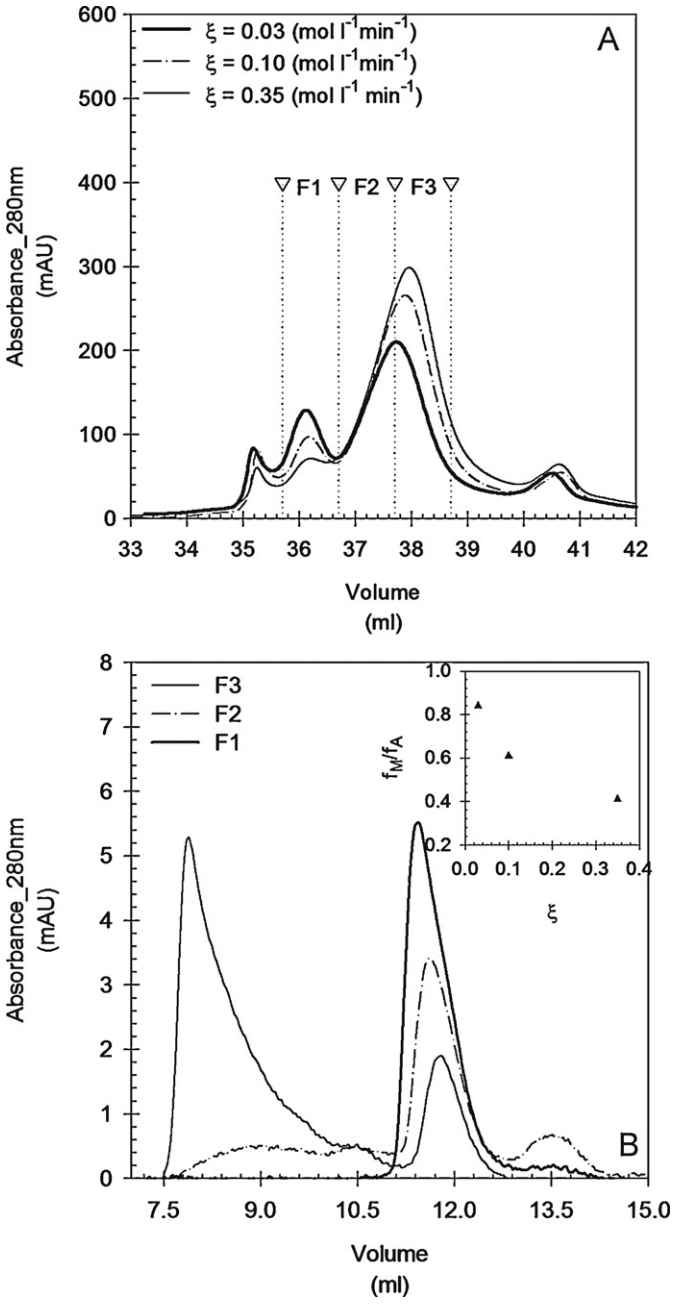

Fig. 7. AExR refolding experiments as a function of the urea gradient slope (ξ). (A) Typical elution profiles of the anion-exchange model system as a function of the urea gradient slope. Solid thick line: $\xi = 0.03\ mol\ l^{-1}\ min^{-1}$; dash–dot line: $\xi = 0.10\ mol\ l^{-1}\ min^{-1}$; solid thin line: $\xi = 0.35\ mol\ l^{-1}\ min^{-1}$. The D&R protein load in these experiments was fixed at 1 mg. (B) SEC analysis of the fractions collected during the AExR experiments. Solid thin line: AExR fraction F3; dash–dot line: AExR fraction F2; solid thick line: AExR fraction F1. Inset: correlation between the fraction of monomers to aggregates ratio (f_M/f_A) and ξ.

Table 5
Performance of the AExR model system as a function of the urea gradient slope (ξ).

[a] ξ	Y_N	$f_{Prot,Rec}$	[b] f_M/f_A
0.35	0.14	0.55	0.41
0.10	0.18	0.57	0.61
0.03	0.20	0.57	0.84

[a] Load = 1 mg protein/ml of packed bed.
[b] This indicator was determined from the SEC analysis of the AExR fractions.

the $f_{Rec,Prot}$ remained practically constant was anticipated, as this indicator strongly depends on the protein load (Table 4, Fig. 4A–C), which was fixed during these experiments. The change in the AExR refolding yield as a function of ξ is reasonably explained by the dependency of the fraction of monomers to aggregates ratio (f_M/f_A) on ξ. This dependency is presented in Table 5 and the inset of Fig. 7B. The data show that f_M/f_A is inversely proportional to ξ, explaining the refolding yield variation. Overall, based on the data gathered it can be concluded that there is a direct link between the AExR yield and the urea gradient, and this link can be quantitatively described by the gradient slope (ξ). Finally, it is important to mention that these experiments do not capture the individual contributions to the magnitude of change in the AExR refolding yield, from the speed of change in urea concentration and the change in residence time of the bound protein, as both are changing with ξ. Eq. (9) shows the relation between the residence time, represented by the duration of the urea gradient block ($t_{UreaGradient}$) (Fig. 1), and ξ. Basically, a shallower (low ξ) or steeper (high ξ) urea gradient not only results in a change in the speed at which the urea concentration is changing, but it also results in a change on the time the protein is bound to the column (a shallower gradient means a longer time and a steeper gradient means a short time). Understanding these individual contributions is important and it is the aim of future work.

$$t_{UreaGradient} = \frac{V_C}{\phi_{v,UreaGradient}} = \frac{1}{\xi}\frac{(C_{Urea,Init} - C_{Urea,End})}{\Delta CV} \quad (9)$$

4. Conclusion

The work presented in this paper described a quantitative analysis of two of the main acknowledged advantages of ion-exchange refolding (IExR), namely the spatial isolation and the controllable change in the chemical composition, attained using a urea gradient. These advantages were described using two descriptors, the fractional surface coverage (θ) and the slope of the urea gradient (ξ). Using these descriptors, the following observations were made: (a) there is a good correlation between fractional mass recovery ($f_{Rec,Prot}$) and θ. This correlation indicated that as θ approaches a certain threshold, the $f_{Rec,Prot}$ will begin to decrease. Basically, as the θ increases the spatial isolation between bound protein molecules decreases, leading to an increase in protein–protein interactions between the bound protein molecules and incoming molecules, resulting in the formation of a tightly bound layer of protein; and (b) this work showed that there is a direct link between the urea gradient and the ion-exchange refolding yield (Y_N), and that this link can be quantitatively described by the urea gradient slope (ξ). Additionally this study shows: (1) that the difference in saturation capacity of an adsorbent (q_S) for a denatured protein and a native protein, can be reasonably explained by their difference in accessible binding surface area; (2) that the protein load does affect the fractional mass recovery ($f_{Rec,Prot}$) and that the magnitude of this effect strongly depends on the loading state of the protein solution (i.e., native, denatured, denatured and reduced (D&R)), and the adsorbent type. Furthermore, the effect of the adsorbent is predominantly related to the nature of the adsorbent's backbone; and (3) that increasing the denatured and reduced (D&R) protein load adversely affect the ion-exchange refolding yield, and this adverse effect could be linked to an increase in the mass fraction of aggregated protein.

Finally, as a consequence of the answers given to the initial questions posed at the beginning of this work, it became evident that significant progress could be made if future studies on ion-exchange protein refolding set to investigate what are the contributions of the physicochemical properties of a given ion-exchange medium, to the performance of the ion-exchange refolding reactor. Such knowledge, would pave the way towards the rational design or selection of an ion-exchange media suitable for the efficient refolding of a target protein.

References

[1] F.R. Schmidt, Appl. Microbiol. Biotechnol. 65 (2004) 363.
[2] K. Terpe, Appl. Microbiol. Biotechnol. 72 (2006) 211.
[3] A.L. Demain, P. Vaishnav, Biotechnol. Adv. 27 (2009) 297.
[4] E.J. Freydell, M. Ottens, M. Eppink, G.V. Dedem, L.V.D. Wielen, Biotechnol. J. 2 (2007) 678.
[5] K. Tsumoto, D. Ejima, I. Kumagai, T. Arakawa, Protein Expres. Purif. 28 (2003) 1.
[6] M. Umetsu, K. Tsumoto, S. Nitta, T. Adschiri, D. Ejima, T. Arakawa, I. Kumagai, Biochem. Biophys. Res. Commun. 328 (2005) 189.
[7] S. Singh, A. Panda, J. Biosci. Bioeng. 99 (2005) 303.
[8] X. Geng, X. Chang, J. Chromatogr. 599 (1992) 185.
[9] Q. Bai, Y. Kong, X.-D. Geng, J. Liq. Chromatogr. Relat. Technol. 26 (2003) 683.
[10] C. Wang, X. Geng, D. Wang, B. Tian, J. Chromatogr. B 806 (2004) 185.
[11] E.J. Freydell, Y. Bulsink, S.H. Van Hateren, L.A.M. van der Wielen, M. Eppink, M. Ottens, Chem. Eng. Sci. 65 (2010) 4701.
[12] B. Batas, J.B. Chaudhuri, Biotechnol. Bioeng. 50 (1996) 16.
[13] H. Rogl, K. Kosemund, W. Kühlbrandt, I. Collinson, FEBS Lett. 432 (1998) 21.
[14] R. Zahn, C. von Schroetter, K. Wüthrich, FEBS Lett. 417 (1997) 400.
[15] M. Langenhof, S.S.J. Leong, L.K. Pattenden, A.P.J. Middelberg, J. Chromatogr. A 1069 (2005) 195.
[16] C. Machold, R. Schlegl, W. Buchinger, A. Jungbauer, J. Biotechnol. 117 (2005) 83.
[17] T.E. Creighton, UCLA Symp. Mol. Cell. Biol. New Ser. 39 (1986) 249.
[18] M. Li, G. Zhang, Z. Su, J. Chromatogr. A 959 (2002) 113.
[19] M. Li, Z. Su, Chromatographia 56 (2002) 33.
[20] M. Li, Z.-G. Su, Biotechnol. Lett. 24 (2002) 919.
[21] Y. Chen, S.S.J. Leong, J. Chromatogr. A 1216 (2009) 4877.
[22] R.E. Canfield, J. Biol. Chem. 238 (1963) 2698.
[23] E.D.B. Clark, D. Hevehan, S. Szela, J. Maachupalli-Reddy, Biotechnol. Prog. 14 (1998) 47.
[24] L.R. Wetter, H.F. Deutsch, J. Biol. Chem. 192 (1951) 237.
[25] T. Ellingsen, O. Aune, J. Ugelstad, S. Hagen, J. Chromatogr. 535 (1990) 147.
[26] J.-C. Janson, Korean J. Chem. Eng. 18 (2001) 149.
[27] B.D. Bowes, H. Koku, K.J. Czymmek, A.M. Lenhoff, J. Chromatogr. A 1216 (2009) 7774.
[28] J. Winter, H. Lilie, R. Rudolph, Anal. Biochem. 310 (2002) 148.
[29] J. Winter, P. Neubauer, R. Glockshuber, R. Rudolph, J. Biotechnol. 84 (2000) 175.
[30] USP27-NF26, US Pharmacopeia (2007) 2.
[31] G. Guiochon, D.G. Shirazi, A. Felinger, A.M. Katti, Fundamentals of Preparative and Nonlinear Chromatography, Academic Press, 2006.
[32] F. Gritti, W. Piatkowski, G. Guiochon, J. Chromatogr. A 978 (2002) 81.
[33] W. Norde, Clin. Mater. 11 (1992) 85.
[34] P. DePhillips, A.M. Lenhoff, J. Chromatogr. A 883 (2000) 39.
[35] Y. Yao, A.M. Lenhoff, J. Chromatogr. A 1126 (2006) 107.
[36] B. Batas, H.R. Jones, J.B. Chaudhuri, J. Chromatogr. A 766 (1997) 109.
[37] A.P.J. Middelberg, Trends Biotechnol. 20 (2002) 437.